https://doi.org/10.5194/egusphere-2024-2943
Preprint. Discussion started: 22 October 2024

Pooled Error Variance and Covariance Estimation of Sparse In Situ Soil Moisture Sensor Measurements in Agricultural Fields in Flanders

Marit G.A. Hendrickx[*1,2], Jan Vanderborght[1,3], Pieter Janssens[1,4,5], Sander Bombeke[6], Evi Matthyssen[7], Anne Waverijn[8], Jan Diels[1,2]

[1] Department of Earth and Environmental Sciences, KU Leuven, Leuven, 3001, Belgium
[2] KU Leuven Plant Institute (LPI), KU Leuven, Leuven, 3001, Belgium
[3] Agrosphere Institute IBG-3, Forschungszentrum Jülich GmbH, Jülich, 52425, Germany
[4] Soil Service of Belgium, Leuven, 3001, Belgium
[5] Department of Biosystems, KU Leuven, Leuven, 3001, Belgium
[6] Proefstation voor de Groenteteelt, Sint-Katelijne-Waver, 2860, Belgium
[7] Praktijkpunt Landbouw Vlaams-Brabant, Herent, 3020, Belgium
[8] Viaverda vzw, Kruishoutem, 9770, Belgium

[*] *Correspondence to*: Marit Hendrickx (marit.hendrickx@kuleuven.be)

Abstract. Accurately quantifying errors in soil moisture measurements from in situ sensors at fixed locations is essential for reliable state and parameter estimation in probabilistic soil hydrological modeling. This quantification becomes particularly challenging when the number of sensors per field or measurement zone (MZ) is limited. When direct calculation of errors from sensor data in a certain MZ is not feasible, we propose to pool systematic and random errors of soil moisture measurements for a specific measurement setup to derive a pooled error covariance matrix that applies across different fields and soil types. In this study, a pooled error covariance matrix was derived from soil moisture sensor measurements and soil moisture sampling campaigns conducted over three growing seasons, covering 93 cropping cycles in agricultural fields with diverse soil textures in Belgium. The MZ soil moisture estimated from soil samples, which showed a small standard error (0.0038 $m^3 m^{-3}$) and which was not correlated between different sampling campaigns since soil samples were taken at different locations, represented the 'true' MZ soil moisture. First, we established a pooled linear recalibration of the TEROS 10 (Meter Group, Inc., USA) manufacturer's sensor calibration function. Then, for each individual sensor as well as for each MZ, we identified systematic deviations and temporally varying residual deviations between the calibrated sensor data and sampling data. The autocovariance of the individual or the MZ-averaged sensor measurement errors was represented by the variance of the systematic deviations across all sensors or MZs whereas the random error variance was calculated from the variance of the pooled residual deviations. The total error variance was equal to the sum of the autocovariance and random error variance. Due to spatial sensor correlation, the variance and autocovariance of MZ-average sensor measurement errors could not be derived from the individual sensor error variances and covariances. The pooled error covariance matrix of the MZ-averaged soil moisture measurements indicated a significant sensor error autocorrelation of 0.518, as the systematic error standard deviation ($\sigma_{\bar{\alpha}} = 0.0327$ $m^3 m^{-3}$) was similar to the random error standard deviation ($\sigma_{\bar{\epsilon}} = 0.0316$ $m^3 m^{-3}$). These results demonstrate that the common assumption of uncorrelated random errors to determine parameter and model prediction uncertainty is not valid when measurements from sparse in situ soil moisture sensors are used to parameterize soil hydraulic models. Further research is required to assess to what extent the error covariances found in this study can be transferred to other areas, and how they impact parameter estimation in soil hydrological modeling.

Main abbreviations: SWC, soil water content; MZ, measurement zone

Keywords: in situ measurements, measurement errors, soil moisture sensor, pooled errors, measurement zone

https://doi.org/10.5194/egusphere-2024-2943
Preprint. Discussion started: 22 October 2024

40 **Graphical abstract**

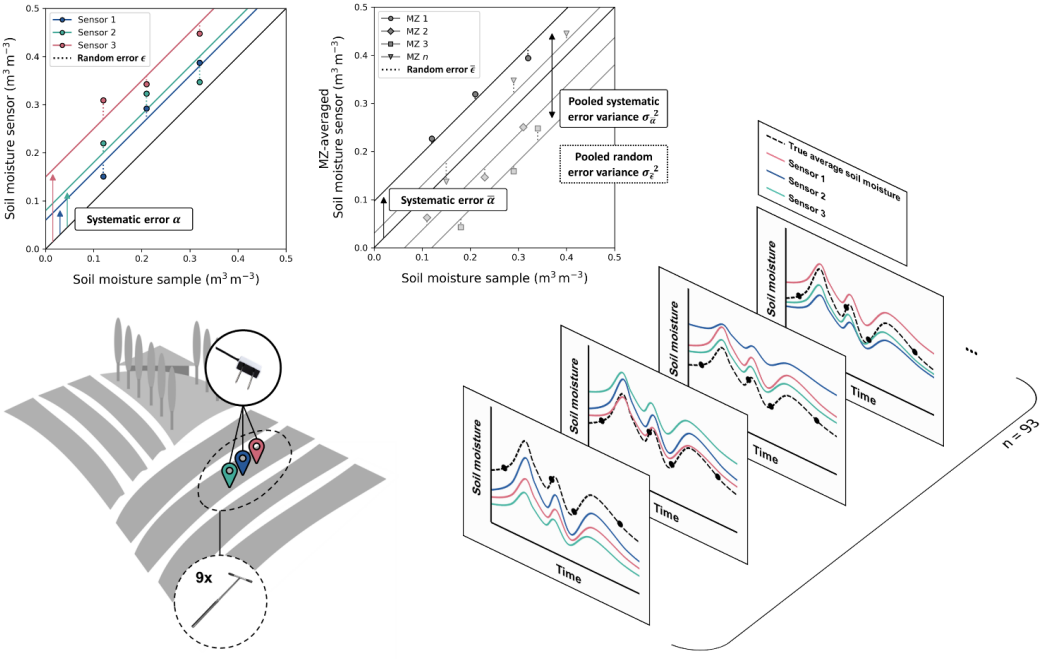

https://doi.org/10.5194/egusphere-2024-2943
Preprint. Discussion started: 22 October 2024

1 Introduction

Soil moisture measurements, such as measurements from in situ soil moisture sensors and sampling, are at the core of soil hydrological modeling, state and parameter estimation by assimilation, model validation, and decision making. However, these soil moisture measurements are subject to multiple sources of uncertainty, introducing systematic and random errors. Accurately quantifying these two types of errors is important to assess the uncertainty of estimated parameters and model predictions since the impact of random errors on this uncertainty vanishes with an increasing number of measurements whereas that of the systematic errors does not. However, this error quantification presents a significant challenge.

Field-scale soil moisture patterns have a strong temporal stability which can be explained by spatial patterns in soil properties and topology (Brocca et al., 2010; Vachaud et al., 1985). As such, individual locations are time-stable and some locations have the time-invariant property to represent the field mean (Vachaud et al., 1985), while other locations consistently deviate from this mean. Several studies have investigated an optimal sampling or sensor network design to represent true soil moisture mean and variability in heterogeneous fields (Brocca et al., 2010; Chaney et al., 2015; Rossini et al., 2021; Wang et al., 2008), but such an optimal measurement design is not always feasible due to practical and budgetary constraints.

In addition to field-scale variability, microscale variability may also substantially impact soil moisture measurements (Hawley et al., 1983), especially point measurements with a small measurement volume. Microscale soil moisture variability may be due to variations in soil particle and pore size, preferential flow (e.g., via biopores from burrowing animals), plant roots, microtopography, soil texture heterogeneity (e.g., clayey or sandy patches), uneven soil compaction, and localized irrigation practices (e.g., drip irrigation). As a result, soil moisture measurements may vary strongly depending on the location of the measurement (Schelle et al., 2013). When soil sampling is used to quantify soil moisture in a measurement zone (MZ) within a field, experimental errors can be minimized by collecting a composite sample from a sufficient number of random locations within that MZ. While the measurement volume of a composite soil sample is large enough to be independent of the microscale variability, a sensor measurement is not and measurement errors may depend on the local positioning of the sensors.

Quantifying measurement errors is trivial when measurements from sufficient locations are available. However, while experimental errors of subsequent soil moisture samplings over time are uncorrelated, such measurements are often temporally sparse. In contrast, using sensors allows for high temporal resolution, but typically only a few sensors are installed within a field often resulting in inadequate spatial coverage. This can lead to a biased mean sensor measurement compared to the true average soil moisture in the MZ, which translates to autocorrelated sensor measurement errors, i.e., errors that are correlated over time. This autocorrelation increases as the systematic error or bias becomes greater relative to the random measurement error. Recently, Hendrickx et al. (2023) demonstrated that soil moisture sensor measurement errors, i.e., the deviations between individual sensors and the true average soil moisture, are strongly correlated over time due to spatial variability and patterns in soil water retention properties.

Information on the spatiotemporal behavior of soil moisture measurements and their errors is especially important in the context of data assimilation and inverse modeling. Previous studies focused on spatial and temporal correlation of soil moisture measurements, as the required spatial density of the measurement network and the assimilation frequency depend on these properties, respectively (De Lannoy et al., 2006). Temporal correlation of soil water content (SWC) represents the persistence of SWC deviations from the long term temporal mean – a concept that is also referred to as ‘soil moisture memory’ (Rahmati et al., 2024). This is related to the temporal dynamics of the meteorological forcings and to water flow in the soil, which depends on soil hydraulic properties. In this study, we are focusing on the temporal correlation of the soil moisture measurement errors, which we define as the deviations of soil moisture measurements from the mean soil moisture in a measurement zone (MZ). This temporal correlation of errors is equal to the ratio of the error covariance to the total error variance and is related to the temporal stability of the spatial variability of soil moisture and thus of a sensor measurement error at a fixed position, rather than on the temporal correlation of the SWC itself. We will refer to this temporal error

https://doi.org/10.5194/egusphere-2024-2943
Preprint. Discussion started: 22 October 2024

correlation as error autocorrelation and will discuss potential implications of spatial correlation of the sensor measurement errors on this error autocorrelation quantification.

The error covariance matrix, which accounts not only for error variance but also error autocorrelation, is essential in data assimilation as it helps to manage uncertainties and correctly attribute weights to measurement errors. Taking both observation and forecast bias into account in data assimilation, and estimating in addition to or even simultaneous with model state variables results in improved estimation results, while neglecting error correlations can lead to significant errors in both the state and bias estimates, which in turn affects the overall model accuracy (Crow and Van Loon, 2006; Pauwels et al., 2013; Pauwels and De Lannoy, 2015). Bayesian methods provide a formal probabilistic framework for incorporating uncertainties and error autocorrelations through the error covariance matrix. In Bayesian inverse modeling, a prior distribution, i.e., of a model state or parameter, can be updated based on uncertain observations. The posterior distribution can be derived by adopting Bayes' theorem (Eq. (1)).

$$p(\boldsymbol{A}|\boldsymbol{B}) = \frac{p(\boldsymbol{A})\,p(\boldsymbol{B}|\boldsymbol{A})}{p(\boldsymbol{B})}\,, \tag{1}$$

where $\boldsymbol{A}$ signifies a vector of model states or parameters, with $p(\boldsymbol{A})$ being the prior probability, while $\boldsymbol{B}$ signifies the observations, with $p(\boldsymbol{A}|\boldsymbol{B})$ being the posterior or conditional probability, $p(\boldsymbol{B}|\boldsymbol{A}) \equiv L(\boldsymbol{A}|\boldsymbol{B})$ being the likelihood of $\boldsymbol{A}$ given $\boldsymbol{B}$, and $p(\boldsymbol{B})$ the marginal probability, which is a normalizing constant.

The (log)likelihood summarizes the errors between model simulations and corresponding observations, and is often used as an objective function. If these errors are uncorrelated and Gaussian distributed, the loglikelihood can be defined by Eq. (2) for heteroscedastic errors (Vrugt, 2016).

$$\mathcal{L}(\boldsymbol{x};\boldsymbol{\mu},\hat{\boldsymbol{\sigma}}^2) = -\frac{n}{2}\ln(2\pi) - \sum_{t=1}^{n}\ln(\hat{\sigma}_t) - \frac{1}{2}\sum_{t=1}^{n}\left(\frac{x_t-\mu_t}{\hat{\sigma}_t}\right)^2\,, \tag{2}$$

where $\boldsymbol{x}$ is a vector with the model simulations (x_t), $\boldsymbol{\mu}$ is a vector with the mean observations (μ_t) with their corresponding standard deviation $\hat{\sigma}_t$ in $\hat{\boldsymbol{\sigma}}$, and n is the number of simulation–observation pairs. When the errors exhibit temporal correlation, the loglikelihood function in Eq. (2) can be expanded by using the full error covariance matrix (Eq. (3)). In this formulation, autocorrelated heteroscedastic errors can be accurately described.

$$\mathcal{L}(\boldsymbol{x};\boldsymbol{\mu},\boldsymbol{\Sigma}) = -\frac{n}{2}\ln(2\pi) - \frac{1}{2}\ln(|\boldsymbol{\Sigma}|) - \frac{1}{2}(\boldsymbol{x}-\boldsymbol{\mu})^{\mathrm{T}}\boldsymbol{\Sigma}^{-1}(\boldsymbol{x}-\boldsymbol{\mu})\,, \tag{3}$$

where $\boldsymbol{\Sigma}$ is the error covariance matrix.

The (log)likelihood function plays a central role as an objective function in statistical modeling techniques, i.e., Bayes classifiers, support vector machines, Bayesian inverse modeling, and Bayesian data assimilation techniques such as an ensemble Kalman filter and particle filter (Wikle and Berliner, 2007). When using sensor measurements at fixed locations, Eq. (3) should be used to account for autocorrelated measurement errors. Residual errors are often both heteroscedastic and autocorrelated in hydrological modeling (Ammann et al., 2019; Evin et al., 2013; Samadi et al., 2018; Yang et al., 2007). However, most studies use Eq. (2), and hence, often make incorrect assumptions on measurement errors. For example, HYDRUS uses the Levenberg-Marquardt parameter estimation approach, which assumes a diagonal error covariance matrix (Šimůnek et al., 2012). Using Eq. (2) is acceptable when an average of a large number of sensors is used (e.g., Steenpass et al. (2010), who used TDR sensors at 36 locations), but not if only a few sensors are available (e.g., Han et al. (2023)). Alternatively, error autocorrelation can be represented by autoregressive models, which have been assessed in several hydrological applications (Engeland and Gottschalk, 2002; Evin et al., 2013; Scharnagl et al., 2015).

When soil moisture is observed and modeled at sub-field or field-scale, limited methods exist to obtain a good estimate of the true mean soil moisture, its errors, and error autocorrelation. A MZ-specific measurement error covariance matrix cannot be derived accurately from a limited number of sensors in a field. Hendrickx et al. (2023) recently proposed a mechanistic error modeling approach to estimate soil moisture error (co)variabilities based on the spatial variability of the water retention curve. However, this method requires detailed soil data from repeated sampling of undisturbed soil cores, which is impractical. To the best of our knowledge, literature on this topic is scarce, hence further research is needed to address this gap.

https://doi.org/10.5194/egusphere-2024-2943
Preprint. Discussion started: 22 October 2024

We propose a pooled error modeling approach, which unifies measurement errors that are observed in multiple fields with an identical measurement setup but with only a limited number of sensors in one field. In this study, a pooled measurement error covariance matrix is quantified based on a considerable dataset of sensor and soil sample data from 93 cropping cycles in agricultural fields in Flanders, Belgium (Sect. 0). This pooled measurement error covariance matrix could then be applied for data assimilation or Bayesian inverse modelling across fields and soil types given the specific measurement setup. First, the pooled sensor calibration is described in Sect. 3. This calibration is applied to all sensor data prior to examining their measurement errors. Then, the error model is described in Sect. 4, and is presented in two ways, i.e., using individual sensor measurements and using field averages. The quantification of the pooled errors is presented (Sect. 5.1), while the consequences of spatial sensor correlation are discussed in Sect. 5.3, and finally, the assumptions of the error model (i.e., data linearity, error normality, error stationarity, spatial consistency and zero cross-correlation) are discussed in-depth in Sect. 5.4.

Table 1 List of symbols and their description

AR	Autocorrelation, i.e., temporal correlation, of measurement errors
MZ	Measurement zone, i.e., a subplot within a field where measurements are taken
S_{mV}	Raw sensor output (mV)
s_{pooled}	Pooled standard deviation of an individual soil moisture sample
SWC	Soil water content ($m^3\ m^{-3}$)
α	Systematic error of an individual sensor
$\bar{\alpha}$	Systematic error of an MZ-averaged sensor measurement
β	Temporally variable process-related deviations between sensor measurements and the true soil moisture that are correlated between sensors
ϵ	Random error of an individual sensor
$\bar{\epsilon}$	Random error of an MZ-averaged sensor measurement
ϵ_{nc}	Non-correlated random error of an MZ-averaged sensor measurement
$\theta_{\mathrm{g,samp}}$	Gravimetric SWC ($kg\ kg^{-1}$) of a soil gouge sample
θ_{sensor}	Calibrated sensor measurement ($m^3\ m^{-3}$) representing the volumetric SWC in the 0-30 cm soil layer
$\theta_{\mathrm{sensor,nocal}}$	Volumetric SWC ($m^3\ m^{-3}$) derived from sensor measurements calibrated with the manufacturer's calibration equation, but not calibrated against soil moisture measurements in the fields
$\theta_{\mathrm{v,samp}}$	Volumetric SWC ($m^3\ m^{-3}$) of a soil gouge sample
ρ_{b}	Dry bulk density ($kg\ m^{-3}$)
ρ_{α}	Temporally stable spatial sensor correlation, i.e., correlation between systematic measurement errors of individual sensors
ρ_{ϵ}	Temporally variable spatial sensor correlation, i.e., correlation between the 'random' errors of individual sensors
σ^2_{samp}	Pooled error variance of composite soil moisture samples
σ^2_{tot}	Pooled total error variance of an individual sensor
$\sigma_{\overline{\mathrm{tot}}}{}^2$	Pooled total error variance of the MZ-averaged sensor measurements
σ^2_{α}	Pooled systematic error variance of an individual sensor
$\sigma_{\bar{\alpha}}{}^2$	Pooled systematic error variance of the MZ-averaged sensor measurements, i.e., pooled error covariance
σ^2_{ϵ}	Pooled random error variance of an individual sensor
$\sigma_{\bar{\epsilon}}{}^2$	Pooled random error variance of the MZ-averaged sensor measurements

2 Study sites and data

Each year during three growing seasons (2021−2023), about 30 agricultural fields for vegetable production were equipped with a sensor module. In every field, soil moisture samples were taken on a regular basis. All fields were located in Flanders, the northern half of Belgium, had an area of 1 to 5 ha, were irrigated using various irrigation methods, and included soil textures ranging from sand to silt. While most of the fields were for commercial production purposes, experimental fields at three research centers were included as well.

https://doi.org/10.5194/egusphere-2024-2943
Preprint. Discussion started: 22 October 2024

Dielectric capacitance soil moisture sensors (TEROS 10, Meter Group, Inc., USA) were used to measure daily volumetric SWCs in the fields. The manufacturer's calibration equation for mineral soils (Eq. (4)) was applied to convert the raw sensor output in mV to volumetric SWC ($m^3\ m^{-3}$) (TEROS 10, 2024).

$$\theta_{\text{sensor,nocal}} = -2.154 + 3.898 \times 10^{-3} \times S_{\text{mV}} - 2.278 \times 10^{-6} \times S_{\text{mV}}^2 + 4.824 \times 10^{-10} \times S_{\text{mV}}^3 , \quad (4)$$

where S_{mV} is the raw sensor output (mV), and $\theta_{\text{sensor,nocal}}$ is the volumetric SWC ($m^3\ m^{-3}$) derived from sensor measurements that were not calibrated against soil moisture measurements in the fields. A list of symbols used in this paper is provided in Table 1.

A sensor module consisted of three TEROS 10 sensors connected to a datalogger equipped with a communication module (Sigfox). The communication module enabled the acquisition and transmission of sensor data to an online server, ensuring real-time online data access. The sensors were installed horizontally at 15 cm depth, with 2 m distance between two sequential sensors within the MZ specified by the farmer.

At the beginning of the growing season, undisturbed Kopecky ring samples (V: 100 cm^3, h: 51 mm) were taken at each study site to determine bulk density. Soil moisture samples (from 2 to 30 cm depth) were taken regularly (every two to four weeks) with a gouge auger at all sites during the growing period, and soil moisture was quantified using the gravimetric method. The volumetric SWC was then calculated based on the gravimetric SWC and bulk density (Eq. (5)).

$$\theta_{\text{v,samp}} = \theta_{\text{g,samp}} \frac{\rho_{\text{b}}}{\rho_{\text{w}}} , \quad (5)$$

where $\theta_{\text{v.samp}}$ is the volumetric SWC ($m^3\ m^{-3}$) and $\theta_{\text{g,samp}}$ is the gravimetric SWC ($kg\ kg^{-1}$) of the gouge samples, ρ_{b} is the dry bulk density ($kg\ m^{-3}$) and ρ_{w} is the mass density of water ($kg\ m^{-3}$).

At all sites, multiple soil moisture samples (nine in commercial fields, six in experimental fields) were collected within a radius of 5 m around the sensors. These samples were generally combined in a composite sample, while at some of the sites, each sample was analyzed individually to obtain an accurate estimate of the soil moisture sample errors (Sect. 4.1).

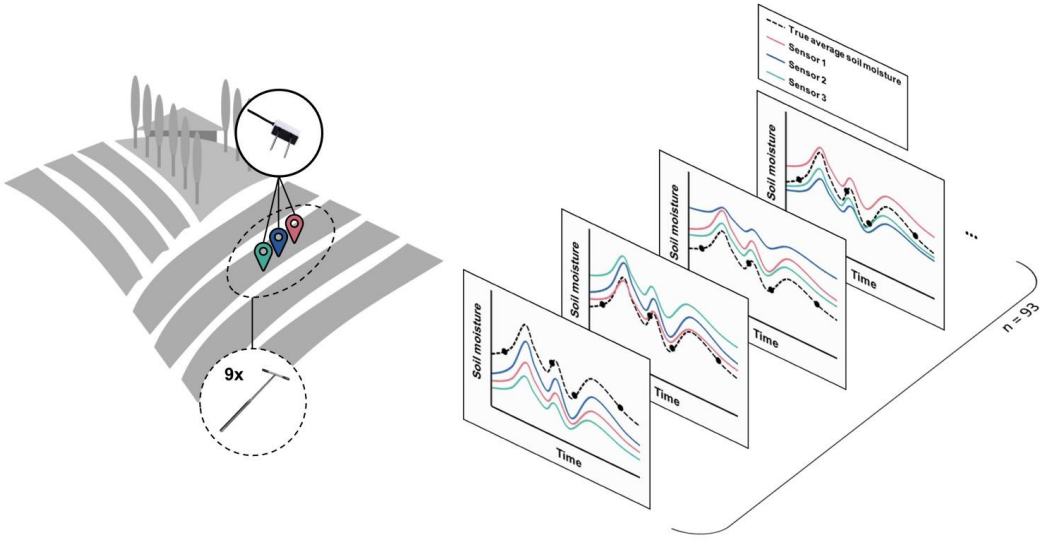

Fig. 1 Illustration of the measurement setup in agricultural fields: The true SWC of the MZ is represented by a composite soil moisture sample of 9 individual gouge auger samples, while three fixed soil moisture sensors measured SWC at 15 cm depth. During three growing seasons (2021−2023), measurement data were collected of 93 cropping cycles.

During data preprocessing, only daily sensor measurements that were complete, with no missing individual sensor data, were retained for error quantification. For fields where two cropping cycles were monitored within the same year, the data were split into two separate cropping cycles as the sensors where removed and reinstalled. Then, cropping cycles that had fewer than two soil moisture sampling events conducted in parallel with the sensor data were excluded from the analysis to ensure

https://doi.org/10.5194/egusphere-2024-2943
Preprint. Discussion started: 22 October 2024

the reliability and accuracy of the error quantification. These preprocessing steps resulted in 93 cropping cycles that were retained for analysis.

3 Pooled sensor calibration

In addition to the manufacturer's calibration equation, a pooled linear recalibration was established to relate the point measurements at 15 cm depth by the sensors with soil moisture samples measuring the whole upper 30 cm layer, so as to obtain sensor measurement data that are representative for this upper soil layer. The composite soil moisture samples of the 30 cm layer were plotted against their corresponding mean sensor measurements at 15 cm depth for all study sites in 2021, 2022 and 2023 (Fig. 2). A bias (ME) of -0.043 $m^3\ m^{-3}$ and an RMSE of 0.058 $m^3\ m^{-3}$ was observed, indicating a significant underestimation of SWC by the sensors.

The calibration curve was fitted using an orthogonal Deming regression, as both the sensor measurements and soil moisture samples are subject to measurement error (Deming, 1938; Ludbrook, 2010). In this regression method, the squares of the perpendicular distances of the calibration points from the regression line are minimized. The prerequisites for this regression method include identical scales of the *x* and *y* variables, similar error variances of the *x* and *y* variables, and a correlation coefficient close to 1, all of which were satisfied for our measurement dataset. The data covered a wide range of SWCs and were strongly correlated with a Pearson correlation of 0.83. The resulting calibration curve (Eq. (6)) had an R^2 of 0.67 and an RMSE of 0.043 $m^3\ m^{-3}$ (Fig. 2). The (perpendicular) residual plot shows randomly scattered residuals and a constant variance, suggesting homoscedasticity (Appendix: Fig. A1).

$$\theta_{\text{sensor}} = -0.006 + 1.26 \times \theta_{\text{sensor,nocal}}\ , \quad (6)$$

where θ_{sensor} ($m^3\ m^{-3}$) is the calibrated sensor measurement representing the volumetric SWC in the 0-30 cm soil layer, and $\theta_{\text{sensor,nocal}}$ ($m^3\ m^{-3}$) is the volumetric SWC that is measured by the non-calibrated sensors at 15 cm depth. The pooled sensor calibration was applied to all sensor data before examining the measurement errors.

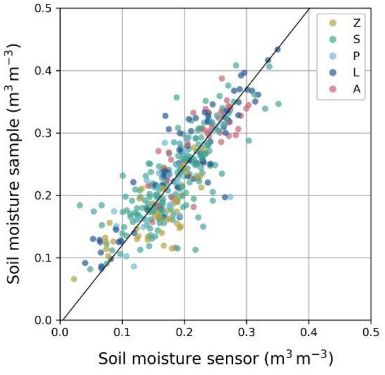

Fig. 2 Mean soil moisture samples, $\theta_{\text{v,samp}}$ ($m^3\ m^{-3}$), in function of mean non-calibrated soil moisture sensor measurements, $\theta_{\text{sensor,nocal}}$ ($m^3\ m^{-3}$), with the pooled sensor calibration curve to obtain sensor measurement data that are representative for the top 30 cm soil layer, as represented by soil moisture samples. The observations are color-coded based on Belgian soil texture class (Z: Sand, S: Loamy sand, P: Light sandy loam, L: Heavy sandy loam, A: Silt loam).

4 Pooled error model approach

4.1 Soil moisture sample measurement errors

The pooled error variance of composite soil moisture samples (σ^2_{samp}) can be determined based on sampling events during which multiple soil moisture samples, i.e., multiple punctures with the gouge auger from the same MZ, are analyzed

https://doi.org/10.5194/egusphere-2024-2943
Preprint. Discussion started: 22 October 2024

individually. First, the sample standard deviation s (for individual samples) can be quantified for each sampling event in each MZ. Then, the pooled standard deviation can be computed to obtain a weighted average of all standard deviations by using Eq. (7), to represent the standard deviation of an individual soil moisture sample.

$$s_{\text{pooled}} = \sqrt{\frac{(n_1-1)s_1^2+(n_2-1)s_2^2+\ldots+(n_p-1)s_p^2}{n_1+n_2+\ldots+n_p-p}}, \quad (7)$$

where s_{pooled} is the pooled standard deviation, p is the number of sampling events, and s_i and n_i are the sample standard deviation and sample size of the i^{th} sampling event, respectively. Finally, the standard error of a composite sample consisting of n individual samples can be computed by dividing the pooled standard deviation by the square root of n, resulting in the pooled error variance of composite soil moisture samples as given by Eq. (8).

$$\sigma_{\text{samp}}^2 = \frac{s_{\text{pooled}}^2}{n}, \quad (8)$$

where n is the number of individual samples in the composite soil sample.

The pooled error model approach assumes zero cross-correlation between the errors of the soil moisture samples and the sensor measurement errors.

4.2 Sensor error model

4.2.1 Individual sensor measurements

When repeated measurements from a sufficiently large number of sensors are available in a MZ, measurement error covariance can be quantified based on the soil moisture measurements directly, between measurement errors at time t_i and t_j as defined by Eq. (9).

$$\text{Cov}(t_i, t_j) = \frac{1}{n-1}\sum_{k=1}^{n}\left(\theta_{\text{sensor}}(t_i,k) - \bar{\theta}(t_i)\right)\left(\theta_{\text{sensor}}(t_j,k) - \bar{\theta}(t_j)\right), \quad (9)$$

where n is the number of sensors in a MZ, $\theta_{\text{sensor}}(t_i,k)$ is the measured SWC by the sensor at location k at time t_i, and $\bar{\theta}(t_i)$ represents the mean SWC at time t_i, which is generally approximated by the average of all sensor measurements.

However, Western and Blöschl (1999) stated that bias is introduced in spatial statistical properties of soil moisture such as covariance and correlation length as the spatial coverage ('extent') of soil moisture measurements decreases. Hence, when a small set of sensors has limited spatial coverage, the variability in the MZ cannot be accurately described by these sensors, which results in an underestimation of the (co)variability, and the mean sensor measurement may be biased compared to the true mean SWC due to local differences. In this case, Eq. (9) may not provide accurate estimates of true SWC error variability and autocorrelation. The limited number of sensors also directly translates to wide confidence intervals on the covariance estimate due to the limited degrees of freedom, e.g., d.f. = 2. Alternatively, a pooled error model approach is proposed that uses higher degrees of freedom by combining information from multiple measurement sites, and is based on a commonly used error model formulation with an additive systematic error term (bias) and a random error term (Eq. (10)). It is important to note that, in order to compute a pooled (co)variance, the model assumes that the (co)variances across different MZs are equal, reflecting spatial consistency.

$$\theta_{\text{sensor},i,k} = \bar{\theta}_i + \alpha_k + \epsilon_{i,k}, \quad (10)$$

where $\theta_{\text{sensor},i,k}$ is the calibrated SWC measured at time i by sensor k (using Eq. (6)), $\bar{\theta}_i$ is the 'true' mean SWC derived from the soil sample measurements at time i, $\alpha_k \sim \mathcal{N}(0, \sigma_\alpha^2)$ is a systematic error that is constant over time of measurements by sensor k, and $\epsilon_{i,k} \sim \mathcal{N}(0, \sigma_\epsilon^2)$ is a random error (Fig. 3a). No multiplicative systematic error is considered here, as this has already been addressed by applying the pooled sensor calibration (Eq. (6)). When there is only a small number and a limited range of soil moisture samples available in each field, a sensor- or MZ-specific slope cannot be derived.

https://doi.org/10.5194/egusphere-2024-2943
Preprint. Discussion started: 22 October 2024

The systematic error (α) of a sensor in a MZ corresponds with its sensor-specific intercept of the relation between the sensor measurement and the 'true' SWC derived from the soil samples. The pooled systematic error variance (σ_α^2) can be calculated from the sensor-specific intercepts of all sensors that are installed in all fields (Eq. (11)).

$$\sigma_\alpha^2 = \mathrm{var}(\alpha) = \frac{1}{S-1}\sum_{k=1}^{S} \alpha_k^2 \,, \tag{11}$$

where S is the number of sensor-specific intercepts.

Then, the pooled random error variance (σ_ϵ^2) is defined as the variance of the sensor measurement errors, ϵ, with respect to their sensor-specific curve ($\hat{\theta}_{i,k} = \bar{\theta}_i + \alpha_k$) using Eq. (12).

$$\sigma_\epsilon^2 = \frac{\sum_{k=1}^{S}\sum_{i=1}^{N_k}(\theta_{\mathrm{sensor},i,k} - \hat{\theta}_{i,k})^2}{\sum_{k=1}^{S} N_k - S} \,, \tag{12}$$

where S is the number of sensor-specific intercepts and N_k is the number of datapoints with sensor k, while $\theta_{\mathrm{sensor},i,k}$ is the calibrated SWC measured by sensor k at time i, and $\hat{\theta}_{i,k}$ is the expected SWC measured by sensor k at time i.

Finally, the total error variance, σ_{tot}^2, of soil moisture measurements by an individual sensor is defined as the sum of the pooled systematic and random error (Eq. (13)).

$$\sigma_{\mathrm{tot}}^2 = \sigma_\alpha^2 + \sigma_\epsilon^2 \,. \tag{13}$$

According to the error model in Eq. (10), the autocovariance of sensor measurement errors is equal to the systematic error variance, σ_α^2. The autocorrelation (AR) between sensor measurement errors at two moments is quantified using Eq. (14). When the sensors are independent from each other, the autocorrelation of the errors of the mean of all sensors in a field will not be different from the autocorrelation of the errors of an individual sensor.

$$\mathrm{AR} = \frac{\sigma_\alpha^2}{\sigma_{\mathrm{tot}}^2} \,. \tag{14}$$

In this error model, the pooled error variance, covariance and autocorrelation are constant in time and the same for all sensors in all fields. As they are pooled over different fields with different soil types, they are expected to be applicable to all fields in the area with a specific measurement setup, i.e., not specific for a particular field or MZ in such a field. Hence, we assume that there are no variations in error variance, covariance, and autocorrelation between different fields, e.g., due to varying soil properties and soil heterogeneity between different fields, nor variations due to varying soil moisture states. Equation (9) requires a sufficient number of sensors (n) to accurately represent field and state-dependent error variances and covariances. The pooled approach, on the other hand, offers the advantage of not being constrained by the number of sensors in a single field, making it suitable for scenarios where sensor deployment is limited.

4.2.2 Averaged sensor measurements

An analogous error model can be formulated for the average of the soil moisture sensor measurements in a MZ with multiple sensors (Eq. (15)).

$$\bar{\theta}_{\mathrm{sensor},i,f} = \bar{\theta}_i + \bar{\alpha}_f + \bar{\epsilon}_{i,f} \,, \tag{15}$$

where $\bar{\theta}_{\mathrm{sensor},i,f}$ is the average SWC measured at time i by the sensors in field f, $\bar{\theta}_i$ is the 'true' mean SWC in the MZ derived from the soil sample measurements, $\bar{\alpha}_f \sim \mathcal{N}(0, {\sigma_{\bar{\alpha}}}^2)$ is a systematic error and $\bar{\epsilon}_{i,f} \sim \mathcal{N}(0, {\sigma_{\epsilon}}^2)$ is a random error (Fig. 3b).

Now, the systematic error ($\bar{\alpha}$) of a MZ corresponds with its MZ-specific intercept, which is the average of the intercepts of the individual sensors in that MZ. The variance of all MZ-specific intercepts corresponds to the pooled systematic error variance, or error covariance (${\sigma_{\bar{\alpha}}}^2$). This pooled systematic error variance is illustrated in Fig. 3b.

$${\sigma_{\bar{\alpha}}}^2 = \mathrm{var}(\bar{\alpha}) = \frac{1}{F-1}\sum_{f=1}^{F} \bar{\alpha}_f^2 \,, \tag{16}$$

where F is the number of fields.

https://doi.org/10.5194/egusphere-2024-2943
Preprint. Discussion started: 22 October 2024

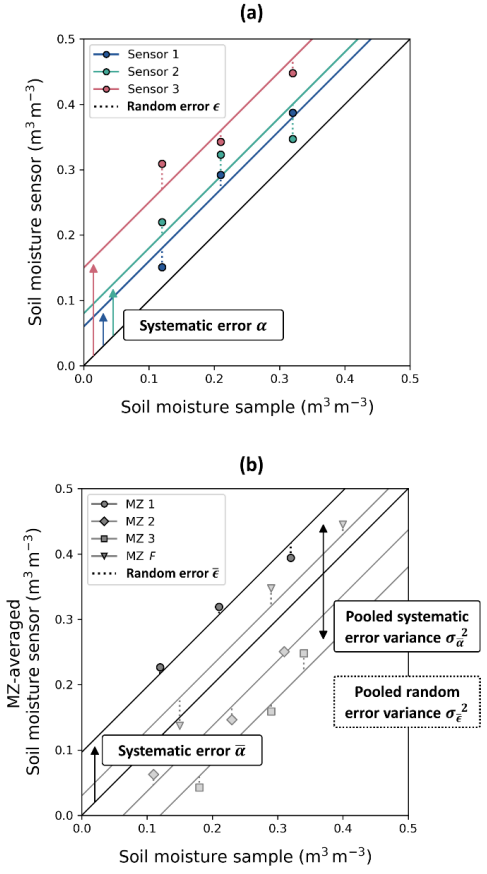

Fig. 3 (a) Individual sensor measurement errors, and (b) MZ-averaged sensor measurement errors with their error variances. The three sensors in (a) correspond to MZ 1 in (b).

The pooled random error variance ($\sigma_{\bar{\epsilon}}{}^2$) is defined as the variance of the error of the average of the sensor measurement errors, $\bar{\epsilon}$, with respect to their MZ-specific curve ($\hat{\theta}_{i,f} = \bar{\theta}_i + \bar{\alpha}_f$) using Eq. (17).

$$\sigma_{\bar{\epsilon}}{}^2 = \frac{\sum_{f=1}^{F}\sum_{i=1}^{N_f}\left(\bar{\theta}_{\mathrm{sensor},i,f} - \hat{\theta}_{i,f}\right)^2}{\sum_{f=1}^{F} N_f - F}, \tag{17}$$

where F is the number of fields, and N_f is the number of datapoints in field f.

The total error variance of the averaged soil moisture measurement, $\sigma_{\overline{\mathrm{tot}}}{}^2$, is defined as the sum of the pooled systematic and random error variances (Eq. (18)):

$$\sigma_{\overline{\mathrm{tot}}}{}^2 = \sigma_{\bar{\alpha}}{}^2 + \sigma_{\bar{\epsilon}}{}^2 . \tag{18}$$

When all sensors in a MZ are (spatially) independent from each other, then the variances of the systematic and random errors of the MZ-averaged soil moisture measurements are related to the respective sensor error variances obtained with Eqs. (11)-(12) as given by Eqs. (19)-(20), respectively.

$$\sigma_{\bar{\alpha}}{}^2 = \frac{\sigma_{\bar{\alpha}}^2}{n}, \tag{19}$$

$$\sigma_{\bar{\epsilon}}{}^2 = \frac{\sigma_{\bar{\epsilon}}^2}{n}, \tag{20}$$

https://doi.org/10.5194/egusphere-2024-2943
Preprint. Discussion started: 22 October 2024

$$\sigma_{\overline{\text{tot}}}{}^2 = \frac{\sigma_{\text{tot}}^2}{n}, \quad (21)$$

where n is the number of sensors in a MZ. The autocorrelation (AR) of the errors of the mean of all sensors in a field is given by Eq. (22). As a result, for independent sensors, the autocorrelation (AR) of the errors of the MZ-averaged soil moisture measurements is equal to that of the individual sensor measurements (Eq. (14)).

$$\text{AR} = \frac{\sigma_{\bar{\alpha}}{}^2}{\sigma_{\overline{\text{tot}}}{}^2}. \quad (22)$$

4.3 Spatial sensor correlation within a MZ

Spatial dependency is inherently present within a MZ as locations that are closer together tend to have more similar soil and plant properties. Therefore, it is best to distribute soil sample and sensor locations well spread across the field or MZ. However, it is not practical to use a set of sensors that are connected to an IoT datalogger via long sensor cables, as they can complicate sensor installation and hinder field operations. In case a small set of sensors with short sensor cables is used and sensor measurement errors in a field are correlated with each other, we underestimate the errors when using Eq. (19)-(20) to infer the systematic and random error variances of field-averaged moisture measurements from systematic and random error variances of the individual sensor measurements.

Spatial sensor correlation can be divided in a temporally stable spatial SWC pattern and a spatial correlation of temporal deviations from the stable SWC pattern. Temporally stable spatial correlation between measurement points that are close to each other within a MZ manifests itself as a systematic deviation of the sensor-specific intercepts (α) within a MZ (illustrated in Fig. 4a) so that $\sigma_{\bar{\alpha}}{}^2 > \frac{\sigma_{\alpha}^2}{n}$, where n is the number of sensors in a MZ. The correlation between the n sensor-specific intercepts in a MZ, ρ_{α}, can be quantified using Eq. (23) (Appendix B). Due to the stable spatial SWC pattern, the systematic deviation of a sensor set of three sensors will depend on the specific location of the sensors within the MZ so that two different sensor sets in the same MZ might have a different systematic deviation from the MZ average SWC (Fig. 4a).

$$\rho_{\alpha} = \frac{n\sigma_{\bar{\alpha}}{}^2 - \sigma_{\alpha}^2}{(n-1)\sigma_{\alpha}^2}. \quad (23)$$

The degree of spatial correlation can be assessed in three ways. The first method involves constructing a semivariogram by quantifying spatial soil moisture variability for different distances. Measured soil moisture variability is expected to increase with distance until soil moisture semivariances stabilize, at which point the measurements can be considered independent and the correlation length, i.e., the range of spatial dependence, can be roughly estimated. The second method compares the variability of the systematic errors α obtained per field ($\sigma_{\bar{\alpha}}{}^2$), i.e., from the average sensor measurements, and the variability of the systematic errors α obtained from the individual sensors (σ_{α}^2). Spatial independence of n sensors within a field implies that the variance of sensor-specific intercepts (σ_{α}^2) equals n times the variance of MZ-specific intercepts ($\sigma_{\bar{\alpha}}{}^2$) (Eq. (19)). Deviations from this condition indicate temporally stable spatial dependence among sensors. The third method analyzes the spatial correlation between the sensor-specific intercepts per MZ.

Analogously, a spatial correlation of random errors of individual sensors, ϵ, corresponds to a spatial correlation of temporal variations in SWC. These temporally varying deviations are related to soil hydrological processes that change soil moisture. Spatial covariance of hydrological processes and of soil properties (soil texture, soil structure, organic matter content, bulk density, and hydraulic conductivity) that define how SWC changes in response to a process result in a spatial covariance of temporal variations in SWC. One can expect that all sensors at 15 cm depth would measure a lower SWC compared to the 'true' SWC of the 0-30 cm soil layer just after a rainfall or irrigation event because precipitation in the top layer has not (yet) been detected by the sensors. Similarly, all sensors would measure a higher SWC compared to the 'true' SWC of the 0-30 cm soil layer in periods with high evaporation from the top soil layer. This results in a random error that varies over time, but part of this variation will be similar for the different sensors in the MZ, i.e., part of the temporal variation of ϵ in Eq. (12) is 'shared' or correlated among sensors. This shared temporal variation of differences between sensor measurements and the true mean

https://doi.org/10.5194/egusphere-2024-2943
Preprint. Discussion started: 22 October 2024

could be represented in the error model by introducing Eq. (10) with a temporally varying term β that is equal for all sensors, while ϵ_{nc} is the remaining non-correlated part of the random error (Eq. (24)).

$$\theta_{\mathrm{sensor},i,k} = \bar{\theta}_i + \alpha_k + \beta_i + \epsilon_{\mathrm{nc},i,k} \,. \tag{24}$$

In contrast to α, which could be interpreted as a temporally fixed deviation related to the spatial variation, the temporally varying β represents process-related deviations between sensor measurements and the true SWC that are correlated between sensors. The temporally variable spatial sensor correlation would manifest itself as a systematic deviation of all sensors in a field at a certain time step (Fig. 4b). When sensor measurements in a field are averaged, the deviation of the spatial average from the true SWC mean that is corrected for the average of the systematic deviations of the sensors, $\bar{\epsilon}$, contains both β and a non-correlated random error ϵ_{nc}:

$$\bar{\epsilon}_{i,f} = \beta_i + \frac{1}{n}\sum_{k=1}^{n} \epsilon_{\mathrm{nc},i,k} \,, \tag{25}$$

so that:

$$\sigma_{\bar{\epsilon}}{}^2 = \sigma_\beta^2 + \frac{\sigma_{\bar{\epsilon},\mathrm{nc}}^2}{n} > \frac{\sigma_\beta^2}{n} + \frac{\sigma_{\bar{\epsilon},\mathrm{nc}}^2}{n} = \frac{\sigma_{\bar{\epsilon}}^2}{n} \,. \tag{26}$$

In a sensor setup with n perfectly correlated sensors, the total random error variance of the field averages ($\sigma_{\bar{\epsilon}}{}^2$) will be equal to the total random error of the individual sensors (σ_ϵ^2) (illustrated in Fig. 4b). The correlation between the 'random' errors of the individual sensors can be quantified using Eq. (27) as derived in Appendix B. This correlation is equal to the ratio of the sensor-correlated 'random' error (co)variance (σ_β^2) to the total 'random' error variance (σ_ϵ^2).

$$\rho_\epsilon = \frac{n\sigma_{\bar{\epsilon}}{}^2 - \sigma_\epsilon^2}{(n-1)\sigma_\epsilon^2} = \frac{\sigma_\beta^2}{\sigma_\epsilon^2} \,. \tag{27}$$

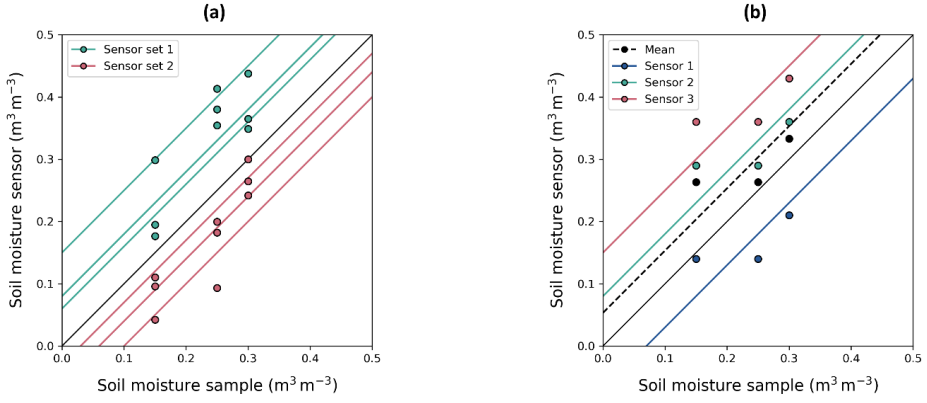

Fig. 4 (a) Illustration of spatial correlation of sensors in a MZ: Sensors that are close together have a similar deviation from the average of the MZ. Two sets of three sensors in the same MZ might have different systematic deviations depending on their location. (b) Illustration of perfect process-related sensor correlation: The three sensors in a single MZ show equal deviations from their sensor-specific curve for a certain soil moisture sampling event.

4.4 Pooled measurement error covariance matrix of averaged soil moisture measurements in a MZ

When all pooled errors are quantified, the pooled measurement error covariance matrix can be built. The measurement error covariance matrix for field f has a size $M \times M$, with M being the sum of the number of (daily) mean sensor measurements in time (N_f) and the number of soil moisture sample events (p) in field f. The error covariance matrix (Fig. 5) contains a $N_f \times N_f$ matrix with the pooled total error variance $\sigma_{\overline{\mathrm{tot}}}{}^2$ (Eq. (18)) on the diagonal and the pooled error covariance $\sigma_{\bar{\alpha}}{}^2$ (Eq. (16)) off-diagonal. The additional p rows and columns represent the uncorrelated soil moisture sampling errors, with the pooled sample error variance σ_{samp}^2 (Eq. (8)) on the diagonal and off-diagonal zeros. The pooled measurement error covariance matrix is by definition invertible and well-conditioned as long as a significant random error is present, i.e., errors are not perfectly autocorrelated.

https://doi.org/10.5194/egusphere-2024-2943
Preprint. Discussion started: 22 October 2024

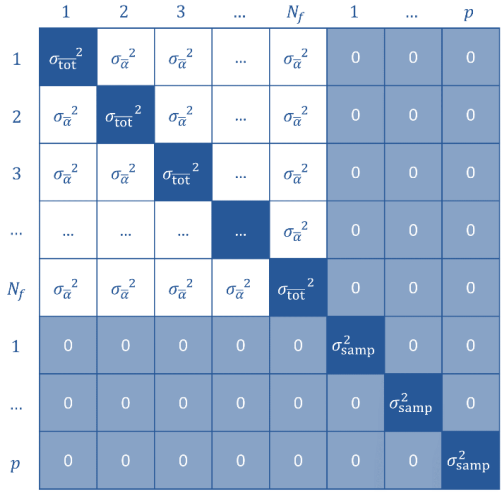

Fig. 5 Error covariance matrix for N_f days of sensor measurements and p soil moisture sampling events in field f.

5 Results and Discussion

5.1 Uncorrelated soil moisture samples

The pooled standard deviation (Eq. (7)) of an individual soil moisture soil sample was 0.0114 m^3 m^{-3}. For nine individual soil samples in a sampling event, the standard error of the mean was 0.0038 m^3 m^{-3} ($\sigma_{\text{samp}}^2 = 0.0000144$). This standard error was small enough to consider these soil moisture samples as reliable reference measurements.

The standard deviation of an individual soil moisture sample was smaller than soil moisture sampling errors found in literature (e.g., Brocca et al., 2010; Famiglietti et al., 2008). However, it is possible that different sampling depths and methods result in different sampling errors. In a particularly heterogeneous field or MZ, a multi-sample analysis is recommended to obtain a more accurate estimate of the soil moisture sample error for that field specifically.

5.2 Sensor measurement error quantification

5.2.1 Systematic errors

In a field equipped with sensor sets in multiple MZs within the field, each sensor set was characterized by a different systematic deviation, α, from their MZ-specific mean SWC measured by the soil moisture samples, of which two MZs are shown in Fig. 6. Moreover, all three sensors in a given MZ showed similar deviations from the composite soil moisture sample in that MZ, e.g., the sensors in MZ 2 all measured a consistently higher SWC compared to the soil moisture samples (Fig. 6b). These similar deviations suggest that the sensors within a MZ are not independent, but rather have spatially correlated measurement errors. Fig. 6a also shows that the autocorrelation of sensor measurement errors remains persistent over time, which is not in line with a classical autoregressive model, where a decay with increasing time lag is typically expected. Moreover, if these error autocorrelations were to be time-variable, autocorrelation would be a function of SWCs or (soil) hydrological events rather than time lag or time itself (Hendrickx et al., 2023).

Furthermore, the sensor data may underestimate the true average SWC in a certain MZ (Fig. 6, MZ 1), while in another MZ, the sensor data may overestimate the true average SWC in the MZ (Fig. 6, MZ 2). This suggests that if the sensor set were installed at a different position within the same MZ, the systematic deviation, α, from its MZ-specific mean SWC would be different (as is also illustrated by sensor removal and reinstallation in Appendix A: Fig. A2). Hence, when more sensors would

https://doi.org/10.5194/egusphere-2024-2943
Preprint. Discussion started: 22 October 2024

be installed within a MZ, expanding spatial coverage and reducing spatial correlation, the systematic error is expected to decrease, likely causing a reduced error autocorrelation (AR).

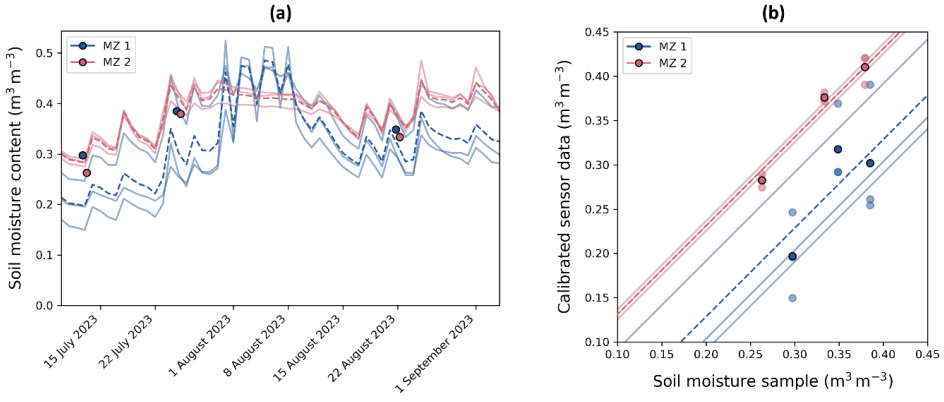

Fig. 6 (a) SWC measured in two MZs within a field with three sensors per MZ. The sensor data were calibrated with the pooled sensor calibration (Eq. (6)), and are plotted along with the MZ-averaged SWC (- - -). (b) Mean SWC (0-30cm) measured with a composite soil sample are plotted against the mean sensor measurements at each location, and their MZ-specific regression line with a slope equal to 1 is shown. The MZ-averaged SWCs and curves are also shown (- - -).

The pooled systematic error variance was quantified for the individual sensors as well as the averaged sensor measurements based on all cropping cycles (Table 2). The individual sensor measurements resulted in 279 sensor-specific intercepts, all based on more than one sampling event, as shown in Fig. 7, which illustrates that measurements by a single sensor may differ consistently over time from the true soil moisture. The standard deviation of these intercepts was 0.03714 $m^3\ m^{-3}$, which corresponded to an error covariance of an individual sensor of $\sigma_{\alpha}^2 = 0.001380$. Under the assumption of sensor independence and for three sensors in a MZ, the error covariance of the average measured soil moisture would be $\sigma_{\bar{\alpha}}^2 = 0.000460$.

Next, the 93 MZ-specific intercepts, all based on the averages of three soil moisture sensor measurements and more than one sampling event, were estimated. The standard deviation of these intercepts was 0.03271 $m^3\ m^{-3}$, which corresponded to an error covariance of $\sigma_{\bar{\alpha}}^2 = 0.001070$, and was considerably larger than the estimate based on the assumption of non-correlated systematic sensor measurement errors.

When analyzing double cropping cycles on a certain field within one year, we see how the mean bias (intercept) shifts after the sensors are removed and reinstalled (Appendix A: Fig. A2). This demonstrates the impact of sensor repositioning on measurement accuracy, highlighting the systematic changes that can occur due to sensor position adjustments.

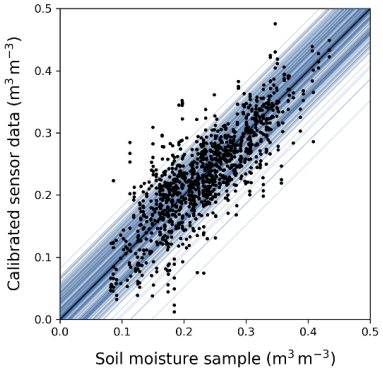

Fig. 7 Intercepts based on individual sensor measurements resulting in 279 sensor-specific curves.

https://doi.org/10.5194/egusphere-2024-2943
Preprint. Discussion started: 22 October 2024

Systematic errors between the mean soil moisture measurement obtained from few sensors with limited spatial coverage and the true mean soil moisture of the MZ may originate from time-persistent spatial differences in soil moisture. Such time-persistent spatial differences may be due to variability in soil properties, water retention, vegetation cover and root distribution (Hendrickx et al., 2023; Schlüter et al., 2013), as well as groundwater depth, topography, and non-equilibrium (Vogel et al., 2010; Schlüter et al., 2012). Brocca et al. (2010) and Vachaud et al. (1985) demonstrated a strong temporal stability of soil moisture variability, indicating a persistent soil moisture pattern over time, which is the main cause of the observed systematic error. Moreover, the dielectric properties of the substrate, influenced by soil properties such as clay content, soil organic matter, bulk density, and soil salinity, may affect the soil moisture measurements of dielectric sensors. Within a MZ, mainly microscale soil moisture variability, resulting from variations in soil particle and pore size, preferential flow, plant roots, microtopography, and localized irrigation practices (e.g. drip irrigation), may significantly impact soil moisture sensor measurements depending on the exact position of the sensor. Finally, systematic errors may also arise due to incorrect sensors installation, e.g., sensors are installed too deep or inserted vertically instead of horizontally, their measurements may be consistently biased. On top of an additive bias, such improper installation could also lead to a multiplicative systematic error, which was not considered in this study.

The difference between the systematic error of individual sensors and the systematic error of averaged sensor measurements was smaller than what would be expected if the time-persistent deviations between the individual sensor measurements and the true SWC would be independent between different sensors. This could be due to spatial correlation of soil moisture that exists within the range of distances between the different sensors in a MZ. As such, sensors that are close together, i.e., sensors that are spatially correlated, will have similar systematic deviations from the true SWC in the MZ due to similar soil and plant properties. Spatial sensor correlation will be further discussed in Sect. 5.3.

5.2.2 Random errors

After estimating the sensor-specific and MZ-specific intercepts, the random errors were quantified for both the individual sensors and the averaged sensor measurements relative to their respective curves (Table 2). The pooled random error variance of the individual sensors (σ_ϵ^2) was quantified based on the sensor measurement errors with respect to their sensor-specific curve using Eq. (12), and resulted in a standard deviation of 0.03440 $m^3\ m^{-3}$ ($\sigma_\epsilon^2 = 0.001183$). The random error variance of the individual sensors was divided by three to obtain the random error variance of the MZ-averages under the assumption of sensor independence, which resulted in ${\sigma_{\bar{\epsilon}}}^2 = 0.000394$. Then, the pooled random error variance of the MZ-averages was quantified based on the measurement errors with respect to their MZ-specific curve using Eq. (17), which resulted in a standard deviation of 0.03159 $m^3\ m^{-3}$ (${\sigma_{\bar{\epsilon}}}^2 = 0.000998$), which was considerably larger than the estimate based on the individual sensors assuming non-correlated random sensor measurement errors.

Fluctuations in environmental conditions, vertical soil moisture (re)distribution and measurement timing affect all sensors equally, resulting in correlated temporal errors across all sensors within a MZ. This process-related sensor correlation will be further discussed in Sect. 5.3.

5.2.3 Total variance and autocorrelation

Finally, the total error variance and autocorrelation were quantified for both the individual sensors and the averaged sensor measurements (Table 2). The pooled total error variance of an individual sensor was 0.002563 ($\sigma_{\text{tot}} = 0.05062\ m^3\ m^{-3}$), and the error autocorrelation (AR) was 0.538. The total error variance of the field averages derived under the assumption of sensor independence using Eq. (21) resulted in $\frac{\sigma_{\text{tot}}^2}{n} = 0.000854$. The pooled total error variance of the average measured SWC using Eq. (18) was ${\sigma_{\overline{\text{tot}}}}^2 = 0.002068$ (${\sigma_{\overline{\text{tot}}}} = 0.04547\ m^3\ m^{-3}$). The pooled systematic error variance ${\sigma_{\bar{\alpha}}}^2$ was similar to the pooled random error variance ${\sigma_{\bar{\epsilon}}}^2$, which caused a strong error autocorrelation of 0.518.

https://doi.org/10.5194/egusphere-2024-2943
Preprint. Discussion started: 22 October 2024

Even though $\sigma_{\overline{\text{tot}}}{}^2$ was significantly different from $\frac{\sigma_{\text{tot}}^2}{n}$, the difference between the AR values was negligibly small, which implies that the random temporal error and the time-invariant systematic error were affected similarly by sensor dependency. The process-related deviations that are temporally varying but correlated among sensors, β, are also affected by spatial dependency, i.e., sensors placed in close proximity are more likely to be at locations with similar soil hydrological process-behavior, characterized by similar soil parameters such as porosity and hydraulic conductivity.

The pooled error autocorrelation found in this study was lower than expected based on previous studies (Hendrickx et al., 2023). A larger spatial soil variability within a MZ would generate a larger systematic deviation of an individual sensor or a group of sensors installed at a specific location in the MZ from the average soil moisture in the MZ. This may be the result of a larger inherent soil heterogeneity, or a larger MZ area. If the random error remains stable while the MZ area expands, the error autocorrelation is likely to increase. In contrast, error autocorrelation of the average sensor measurement is expected to decrease with decreasing spatial sensor correlation. Hence, as sensors are located further apart, spatial sensor correlation decreases resulting in a decrease in error autocorrelation. If the sensors are not biased inherently but their bias is position-dependent as was the case here, the bias of the average sensor measurement will decrease with an increasing number and broader coverage of sensors, again resulting in a decrease in error autocorrelation. The previous study of (Hendrickx et al., 2023) assessed error autocorrelations of the deviations of an individual sensor compared to the average sensor measurement in the field, which was much larger than a MZ in this study, and found error autocorrelations close to 1, as could be expected due to the larger systematic deviations at field scale compared to MZ scale and smaller random errors due to a one-on-one comparison of sensor time series instead of soil moisture samples with a different measurement volume.

The standard deviation of the soil moisture sample mean of nine subsamples ($\sigma_{\text{samp}} = 0.0038$ m^3 m^{-3}) was 12 times smaller than the total error standard deviation of a mean sensor measurement from three sensors ($\sigma_{\overline{\text{tot}}} = 0.04547$ m^3 m^{-3}, Table 2), which would result in a much larger weight of the soil moisture samples in a data assimilation context.

Table 2 Summary of error variances and standard deviations derived from individual and averaged sensor measurements, with a number of N = 3×375 datapoints.

	Individual sensor (Eqs. (10)-(14))	**MZ-averaged assuming spatial sensor independence (Eqs. (19)-(21))**	**MZ-averaged (Eqs. (15)-(18))**
Number of intercepts	279	279	93
Systematic error σ_α^2 (σ_α)	0.001380 (0.03714 m^3 m^{-3})	0.000460 (0.02144 m^3 m^{-3})	0.001070 (0.03271 m^3 m^{-3})
Random error σ_ϵ^2 (σ_ϵ)	0.001183 (0.03440 m^3 m^{-3})	0.000394 (0.01986 m^3 m^{-3})	0.000998 (0.03159 m^3 m^{-3})
Total error σ_{tot}^2 (σ_{tot})	0.002563 (0.05062 m^3 m^{-3})	0.000854 (0.02923 m^3 m^{-3})	0.002068 (0.04547 m^3 m^{-3})
AR	0.5383	0.5383	0.5176
σ_β^2 (Eq. (27))	0.000905 (0.03008 m^3 m^{-3})	NA	NA
$\sigma_{\epsilon,\text{nc}}^2$	0.000279 (0.01669 m^3 m^{-3})	NA	NA

5.3 Spatial sensor correlation assessment

The degree of temporally stable spatial correlation was assessed by performing numerical calculations and spatial analysis on the systematic errors. As the variance of the sensor-specific intercepts (σ_α^2) was significantly smaller than three times the variance of the MZ-specific intercepts ($\sigma_{\bar{\alpha}}{}^2$), the sensors could not be considered spatially independent. The correlation coefficient ρ_α was 0.6554 (Eq. (23)), indicating strong spatial correlation. Additionally, the intercepts of the three sensors in

https://doi.org/10.5194/egusphere-2024-2943
Preprint. Discussion started: 22 October 2024

one field showed strong positive correlations with an average Pearson correlation of 66.5% (Appendix A: Fig. A3). The construction and assessment of a small-scale semivariogram can be found in Supplementary Materials (S1).

The process-related sensor correlation was quantified by comparing the random error variance of the individual sensors (σ_ϵ^2) and the random error variance based on the average of the three sensors ($\sigma_{\bar{\epsilon}}{}^2$). If the random errors of the sensors were independent, $\frac{\sigma_\epsilon^2}{n}$ would be equal to $\sigma_{\bar{\epsilon}}{}^2$, which was not the case. The correlation coefficient ρ_ϵ was 0.7646 (Eq. (27)), which resulted in $\sigma_\beta^2 = 0.000905$ ($\sigma_\beta = 0.03008$ $m^3\,m^{-3}$). This means that only 24% of the total 'random' error was sensor-independent, and assuming sensor independence would result in inaccurate error estimates.

5.4 Assumptions

First of all, the pooled error model approach assumes **linearity** between the true soil moisture contents and the soil moisture contents derived from the sensor measurements with the manufacturer's calibration function. The (perpendicular) residual plot of the pooled linear sensor calibration shows randomly scattered residuals (Appendix: Fig. A1), while the composite soil moisture samples, representing the true soil moisture, and the mean sensor measurements showed a very high correlation of 83%, both suggesting that the linearity assumption is valid. Additionally, second-, third- and fourth-degree polynomial regression models were compared with a linear regression model using the Akaike Information Criterion (AIC), which suggested that the linear model would be the most appropriate choice (Appendix A: Fig. A4).

Secondly, the pooled error model approach assumes **error stationarity and error orthogonality**, i.e., error variances do not change over time, and are therefore also independent of the soil moisture state. Previous studies have, however, shown that spatial soil moisture variability is dependent on the mean soil moisture state (Albertson and Montaldo, 2003; Famiglietti et al., 2008; Hendrickx et al., 2023; Manns et al., 2014; Pan and Peters-Lidard, 2008; Rosenbaum et al., 2012; Schlüter et al., 2013; Teuling and Troch, 2005; Vereecken et al., 2007). Nonetheless, we argue that these assumptions are acceptable during the growing season in an irrigated field as the temporal soil moisture range in such a field will likely be narrow. If the error model were to consider a multiplicative systematic error, the errors would depend on the soil moisture state, i.e., errors would be non-orthogonal. Furthermore, dynamic errors that are independent from soil moisture state might occur when soil properties such as bulk density and field capacity change over time (Jirků et al., 2013).

Additionally, the pooled error model approach assumes **spatial consistency**, i.e., the pooled total error variance ($\sigma_{\overline{tot}}{}^2$) and the pooled error covariance ($\sigma_{\bar{u}}{}^2$) are considered to apply for all fields and all soils in the area in which data were collected in a set of fields well-spread over that area, which implies that we regard the MZs in the different fields over the different years as having equal spatial soil moisture variability. We argue that this assumption is acceptable for MZs of about 80 m², which is smaller than the scale over which significant variations in soil texture, soil properties, topography etc. may occur within a field. Therefore, the variability that we consider is related to microscale variations. Furthermore, we focused on fields that were regularly tilled and harrowed which also reduces spatial variations and differences in variations between fields. Whether the results are also applicable to grasslands or no-till fields would be an interesting future research topic. Moreover, the irrigation method applied during a cropping cycle may impact systematic deviations of the sensors compared to the composite soil moisture samples. As discussed in Supplementary Materials (S2), a pooled error model for a specific irrigation method could result in a more accurate error estimation, but would require an extensive dataset for that specific irrigation method.

When deriving the errors of the MZ-averages from the errors of individual sensors (Eq. (19)-(20)), **sensor independence** is typically assumed. The process-related sensor correlation (impacting random errors) and the spatial correlation (impacting systematic errors) found in this study were 76% and 66%, respectively (Sect. 5.3). The strong correlations that were observed suggest that assuming sensor independence would be incorrect, and the errors of the MZ averages should be computed directly based on the average measurements using Eqs. (15)-(18). Spatial correlation could be reduced by obtaining larger spatial

https://doi.org/10.5194/egusphere-2024-2943
Preprint. Discussion started: 22 October 2024

coverage, e.g., by installing more sensors and by positioning the sensors further apart. Reducing the spatial correlation is however not required as long as it is accounted for in the error model and error covariance matrix.

Furthermore, the pooled error model approach assumes **zero cross-correlation** between the errors of the soil moisture samples and the sensor measurement errors. This assumption was satisfied as the individual soil moisture samples were taken within a radius of 5 m around the sensors and at different locations each time, and they sample different soil volumes. Additionally, it is important to note that the sensor data in a specific field are not calibrated with the MZ-specific samples, but instead are calibrated with the pooled sensor calibration which is based on all fields, ensuring this measurement error independence.

Finally, the error models (Eq. (10) and (15)) and the loglikelihood function defined by Eq. (2) or (3) assume **normally distributed errors**. A normal QQ plot with acceptable heavy tails supports the assumption of normally distributed errors (Appendix A: Fig. A5), while the distributions of the sensor-specific intercepts substantiate the normal distribution of the systematic errors (Appendix A: Fig. A3).

6 General discussion and Conclusions

In this study, the approach was illustrated using soil moisture measurement data from 93 cropping cycles in agricultural fields across Flanders, which were used to quantify the pooled error variance, error covariance, and error autocorrelation of daily soil moisture sensor data. The pooled results apply to a sensor setup with three TEROS 10 sensors that are located close together within a MZ of about 80 m², and apply to fields in the area of Flanders with soil textures ranging from sand to silt.

While this paper focusses on error modeling in soil moisture sensing, the proposed measurement error modeling approach is applicable in various contexts characterized by (1) spatial heterogeneity impacting point measurements, (2) continuous measurements at fixed locations with few repetitions and limited spatial extent due to practical constraints and cost considerations, and (3) reference measurements representing the true average of a MZ. Such measurement setups are prevalent across diverse domains and applications, including but not limited to environmental monitoring, (agro)geophysical monitoring, water quality monitoring, and agricultural management. For example, a stem water potential sensor (e.g., FloraPulse) can be considered the equivalent of a soil moisture sensor, providing automated high-frequency readings but being limited to only a few sensors. Manual stem water potential measurements are the equivalent of manual soil moisture sampling, where measurements on a sufficient number of leaves in the plot can provide a reliable average, but the process is too labor-intensive to perform frequently. Similarly, sap flow sensors, which provide high-frequency data but are expensive and show variability between trees and locations on a tree stem, need to be calibrated with independent observations of transpiration. This calibration can be achieved through longer-term observations of water balance components over several weeks for a MZ, yielding only a few data points over time. In water quality monitoring, multi-parameter sensors for surface water, which are expensive but provide high-frequency data, must be complemented with manual water sampling and laboratory analysis. In agrogeophysical monitoring, methods such as electrical resistivity tomography (ERT) or electromagnetic induction (EMI) are often used to map soil moisture variability across agricultural fields. These methods provide spatially extensive snapshots of subsurface conditions, but they typically require calibration with point measurements, such as soil moisture sensors, to improve accuracy. The pooled sensor calibration and the MZ-specific systematic deviations between the calibrated sensor data and (unbiased) sampling data found in this study indicate that it is essential to consider potential biases of the point-based sensor measurements relative to the true values when using sparse sensor networks to calibrate these geophysical measurements. Similar to the discrepancy between the soil moisture sample of the 30 cm layer and the point measurement of the sensor at 15 cm depth, the point measurement might not be representative for the measurement resolution (both vertical and horizontal) of the geophysical measurement.

The proposed pooled error approach initially requires an extensive measurement dataset, but minimizes MZ-specific measurement requirements. This approach could also be applied to identify measurement errors at larger scales, such as

https://doi.org/10.5194/egusphere-2024-2943
Preprint. Discussion started: 22 October 2024

management zone or field level. This means that, rather than requiring an extensive sensor network in each field or management zone, only few sensors are required in combination with temporally sparse reference measurements. Even with practical and budgetary limitations, this approach permits to accurately estimate soil moisture measurement errors, both systematic and random, and to correctly allocate weight and confidence to different types of measurements. For example, in Bayesian model state and parameter estimation, independent uncorrelated soil moisture samples with a low uncertainty may have a significant impact on model bias reduction when sensor measurement errors are highly autocorrelated. A limitation of this approach is the assumption that all MZs have equal local heterogeneity, which might not always hold true. However, overcoming this limitation would require a denser measurement network in each field, which is exactly what we are trying to avoid. Furthermore, geophysical methods such as ERT and EMI can be applied to quantify spatial variability in a field, but this is typically done only once per crop cycle, often at the start before the crop is established. Integrating these spatial geophysical data with in-situ point measurements can enhance the robustness of parameter estimation in soil hydrological models by providing higher data accuracy and appropriate error propagation. Such joint datasets offer the advantage of capturing both spatial and temporal variations in soil moisture, which are critical for effective irrigation management. This also raises the question of whether a sparse sensor network within one management zone can be used to extrapolate dynamics to other management zones, or if a MZ is required in each management zone. Additionally, it is important to note that sensor measurements in different MZs or management zones within a field could exhibit different spatial patterns compared to the actual conditions and geophysical observations due to varying biases (α) between sensors and ground-truth (e.g., see Fig. 6).

In the context of Bayesian model state or parameter estimation, the accuracy of the error estimates will also significantly impact optimization results, including the uncertainty estimate on the model state or parameter, as inaccurate error estimate will propagate through Bayesian inference. Additionally, adoption of the pooled error approach yields an error covariance matrix that is invertible and well-conditioned. This computational attribute holds particular significance in likelihood computation procedures, ensuring numerical stability and facilitating accurate statistical inference.

To conclude, the pooled error modeling approach facilitates low-density in situ sensor measurement networks while still being able to estimate soil moisture variability and error autocorrelation by assessing MZ-specific biases and random errors. This approach is particularly relevant for agrogeophysical studies, where understanding soil moisture dynamics and their uncertainty is critical for decision-making in agriculture. Neglection of error autocorrelation is a common but incorrect assumption when measurements have limited spatial coverage, as was illustrated by the significant AR of 0.518 found in this study. Future research is needed to evaluate the impact of this pooled error model and uncorrelated soil moisture samples on parameter estimation in Bayesian soil hydrological modeling. Additional work is required to test if the results, i.e., the error variances and autocorrelation found in this study, are applicable in other regions, for different land uses, or alternative setups.

Acknowledgements. This work was funded by the Research Foundation Flanders (FWO fellowship 1S20822N). The study sites were monitored in the context of a project funded by Flanders innovation & entrepreneurship (VLAIO project HBC.2018.2201). We acknowledge the support of the Soil Service of Belgium, who collected the field data, as well as all research centers in Flanders as partners (*Provinciaal Proefcentrum voor de Groenteteelt Oost-Vlaanderen* (PCG) – now Viaverda – , *Proefstation voor de Groenteteelt* (PSKW), *Praktijkpunt Landbouw Vlaams-Brabant*). **AI statement:** In the preparation of this manuscript, AI tools were used for enhancing the readability and quality of the text.

https://doi.org/10.5194/egusphere-2024-2943
Preprint. Discussion started: 22 October 2024

References

Albertson, J. D. and Montaldo, N.: Temporal dynamics of soil moisture variability: 1. Theoretical basis, Water Resour. Res., 39, https://doi.org/10.1029/2002WR001616, 2003.

Ammann, L., Fenicia, F., and Reichert, P.: A likelihood framework for deterministic hydrological models and the importance of non-stationary autocorrelation, Hydrol. Earth Syst. Sci, 23, 2147–2172, https://doi.org/10.5194/hess-23-2147-2019, 2019.

Brocca, L., Melone, F., Moramarco, T., and Morbidelli, R.: Spatial-temporal variability of soil moisture and its estimation across scales, Water Resour. Res., 46, https://doi.org/https://doi.org/10.1029/2009WR008016, 2010.

Chaney, N. W., Roundy, J. K., Herrera-Estrada, J. E., and Wood, E. F.: High-resolution modeling of the spatial heterogeneity of soil moisture: Applications in network design, Water Resour. Res., 51, 619–638, https://doi.org/10.1002/2013WR014964, 2015.

Crow, W. T. and Van Loon, E.: Impact of Incorrect Model Error Assumptions on the Sequential Assimilation of Remotely Sensed Surface Soil Moisture, J. Hydrometeorol., 7, 421–432, https://doi.org/10.1175/JHM499.1, 2006.

Deming, W. E.: Statistical Adjustment of Data, John Wiley & Sons, New York, 1938.

Engeland, K. and Gottschalk, L.: Bayesian estimation of parameters in a regional hydrological model, Hydrol. Earth Syst. Sci., 6, 883–898, 2002.

Evin, G., Kavetski, D., Thyer, M., and Kuczera, G.: Pitfalls and improvements in the joint inference of heteroscedasticity and autocorrelation in hydrological model calibration, Water Resour. Res., 49, 4518–4524, https://doi.org/10.1002/WRCR.20284, 2013.

Famiglietti, J. S., Ryu, D., Berg, A. A., Rodell, M., Jackson, T. J., Famiglietti, C. :, Ryu, D., Berg, A. A., Rodell, M., and Jackson, T. J.: Field observations of soil moisture variability across scales, Water Resour. Res., 44, https://doi.org/10.1029/2006WR005804, 2008.

Han, F., Hu, Z., Chen, N., Wang, Y., Jiang, J., and Zheng, Y.: Assimilating Low-Cost High-Frequency Sensor Data in Watershed Water Quality Modeling: A Bayesian Approach, Water Resour. Res., 59, e2022WR033673, https://doi.org/10.1029/2022WR033673, 2023.

Hawley, M. E., Jackson, T. J., and McCuen, R. H.: Surface soil moisture variation on small agricultural watersheds, J. Hydrol., 62, 179–200, https://doi.org/10.1016/0022-1694(83)90102-6, 1983.

Hendrickx, M. G. A., Diels, J., Janssens, P., Schlüter, S., and Vanderborght, J.: Temporal covariance of spatial soil moisture variations: A mechanistic error modeling approach, Vadose Zo. J., e20295, https://doi.org/10.1002/VZJ2.20295, 2023.

Jirků, V., Kodešová, R., Nikodem, A., Mühlhanselová, M., and Žigová, A.: Temporal variability of structure and hydraulic properties of topsoil of three soil types, Geoderma, 204–205, 43–58, https://doi.org/10.1016/J.GEODERMA.2013.03.024, 2013.

De Lannoy, G. J. M., Verhoest, N. E. C., Houser, P. R., Gish, T. J., and Van Meirvenne, M.: Spatial and temporal characteristics of soil moisture in an intensively monitored agricultural field (OPE3), J. Hydrol., 331, 719–730, https://doi.org/10.1016/J.JHYDROL.2006.06.016, 2006.

Ludbrook, J.: Linear regression analysis for comparing two measurers or methods of measurement: But which regression?, Clin. Exp. Pharmacol. Physiol., 37, 692–699, https://doi.org/https://doi.org/10.1111/j.1440-1681.2010.05376.x, 2010.

Manns, H. R., Berg, A. A., Bullock, P. R., and Mcnairn, H.: Impact of soil surface characteristics on soil water content variability in agricultural fields, Hydrol. Process., 28, 4340–4351, https://doi.org/10.1002/hyp.10216, 2014.

TEROS 10: http://publications.metergroup.com/Manuals/20788_TEROS10_Manual_Web.pdf, last access: 21 May 2024.

Pan, F. and Peters-Lidard, C. D.: On the Relationship Between Mean and Variance of Soil Moisture Fields1, JAWRA J. Am. Water Resour. Assoc., 44, 235–242, https://doi.org/10.1111/J.1752-1688.2007.00150.X, 2008.

Pauwels, V. R. N. and De Lannoy, G. J. M.: Error covariance calculation for forecast bias estimation in hydrologic data assimilation, Adv. Water Resour., 86, 284–296, https://doi.org/10.1016/J.ADVWATRES.2015.05.013, 2015.

Pauwels, V. R. N., De Lannoy, G. J. M., Hendricks Franssen, H.-J., and Vereecken, H.: Simultaneous estimation of model state variables and observation and forecast biases using a two-stage hybrid Kalman filter, Hydrol. Earth Syst. Sci, 17, 3499–3521, https://doi.org/10.5194/hess-17-3499-2013, 2013.

Rahmati, M., Amelung, W., Brogi, C., Dari, J., Flammini, A., Bogena, H., Brocca, L., Chen, H., Groh, J., Koster, R. D., McColl, K. A., Montzka, C., Moradi, S., Rahi, A., Sharghi S., F., and Vereecken, H.: Soil Moisture Memory: State-Of-The-Art and the Way Forward, Rev. Geophys., 62, https://doi.org/10.1029/2023RG000828, 2024.

https://doi.org/10.5194/egusphere-2024-2943
Preprint. Discussion started: 22 October 2024

Rosenbaum, U., Bogena, H. R., Herbst, M., Huisman, J. A., Peterson, T. J., Weuthen, A., Western, A. W., and Vereecken, H.: Seasonal and event dynamics of spatial soil moisture patterns at the small catchment scale, Water Resour. Res., 48, https://doi.org/10.1029/2011WR011518, 2012.

Rossini, P. R., Ciampitti, I. A., Hefley, T., and Patrignani, A.: A soil moisture-based framework for guiding the number and location of soil moisture sensors in agricultural fields, Vadose Zo. J., 20, e20159, https://doi.org/10.1002/VZJ2.20159, 2021.

Samadi, S., Tufford, D. L., and Carbone, G. J.: Estimating hydrologic model uncertainty in the presence of complex residual error structures, Stoch. Environ. Res. Risk Assess., 32, 1259–1281, https://doi.org/10.1007/S00477-017-1489-6/FIGURES/11, 2018.

Scharnagl, B., Iden, S. C., Durner, W., Vereecken, H., and Herbst, M.: Inverse modelling of in situ soil water dynamics: accounting for heteroscedastic, autocorrelated, and non-Gaussian distributed residuals, Hydrol. Earth Syst. Sci. Discuss., 12, 2155–2199, https://doi.org/10.5194/hessd-12-2155-2015, 2015.

Schelle, H., Durner, W., Schlüter, S., Vogel, H.-J., and Vanderborght, J.: Virtual Soils: Moisture Measurements and Their Interpretation by Inverse Modeling, Vadose Zo. J., 12, vzj2012.0168, https://doi.org/10.2136/vzj2012.0168, 2013.

Schlüter, S., Vanderborght, J., and Vogel, H. J.: Hydraulic non-equilibrium during infiltration induced by structural connectivity, Adv. Water Resour., 44, 101–112, https://doi.org/10.1016/J.ADVWATRES.2012.05.002, 2012.

Schlüter, S., Vogel, H.-J., Ippisch, O., and Vanderborght, J.: Combined Impact of Soil Heterogeneity and Vegetation Type on the Annual Water Balance at the Field Scale, Vadose Zo. J., 12, https://doi.org/10.2136/vzj2013.03.0053, 2013.

Šimůnek, J., Van Genuchten, M. T., and Šejna, M.: HYDRUS: Model Use, Calibration, and Validation, Trans. ASABE, 55, 1261–1274, 2012.

Steenpass, C., Vanderborght, J., Herbst, M., Šimůnek, J., and Vereecken, H.: Estimating Soil Hydraulic Properties from Infrared Measurements of Soil Surface Temperatures and TDR Data, Vadose Zo. J., 9, 910–924, https://doi.org/10.2136/VZJ2009.0176, 2010.

Teuling, A. J. and Troch, P. A.: Improved understanding of soil moisture variability dynamics, Geophys. Res. Lett., 32, 1–4, https://doi.org/10.1029/2004GL021935, 2005.

Vachaud, G., Silans, A. P. De, Balabanis, P., and Vauclin, M.: Temporal Stability of Spatially Measured Soil Water Probability Density Function, Soil Sci. Soc. Am. J., 49, 822–828, https://doi.org/10.2136/SSSAJ1985.03615995004900040006X, 1985.

Vereecken, H., Kamai, T., Harter, T., Kasteel, R., Hopmans, J., and Vanderborght, J.: Explaining soil moisture variability as a function of mean soil moisture: A stochastic unsaturated flow perspective, Geophys. Res. Lett., 34, https://doi.org/10.1029/2007GL031813, 2007.

Vogel, H. J., Weller, U., and Ippisch, O.: Non-equilibrium in soil hydraulic modelling, J. Hydrol., 393, 20–28, https://doi.org/10.1016/J.JHYDROL.2010.03.018, 2010.

Vrugt, J. A.: Markov chain Monte Carlo simulation using the DREAM software package: Theory, concepts, and MATLAB implementation, Environ. Model. Softw., 75, 273–316, https://doi.org/https://doi.org/10.1016/j.envsoft.2015.08.013, 2016.

Wang, C., Zuo, Q., and Zhang, R.: Estimating the necessary sampling size of surface soil moisture at different scales using a random combination method, J. Hydrol., 352, 309–321, https://doi.org/10.1016/J.JHYDROL.2008.01.011, 2008.

Western, A. W. and Blöschl, G.: On the spatial scaling of soil moisture, J. Hydrol., 1999.

Wikle, C. K. and Berliner, L. M.: A Bayesian tutorial for data assimilation, Phys. D Nonlinear Phenom., 230, 1–16, https://doi.org/10.1016/J.PHYSD.2006.09.017, 2007.

Yang, J., Reichert, P., Abbaspour, K. C., and Yang, H.: Hydrological modelling of the Chaohe Basin in China: Statistical model formulation and Bayesian inference, J. Hydrol., 340, 167–182, https://doi.org/10.1016/J.JHYDROL.2007.04.006, 2007.

https://doi.org/10.5194/egusphere-2024-2943
Preprint. Discussion started: 22 October 2024

Appendix A: Supplementary figures

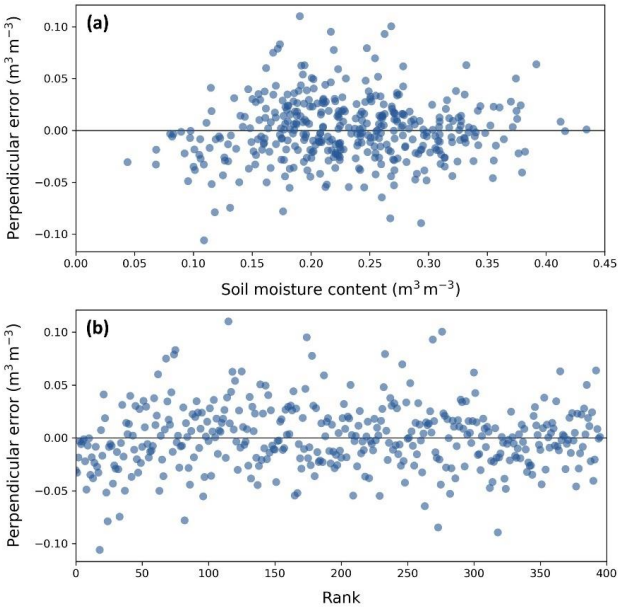

Fig. A1 Perpendicular residuals after applying the orthogonal Deming regression to the sensor data (Eq. (6), Fig. 2), as a function of SWC (a), and as a function of SWC rank (b).

660

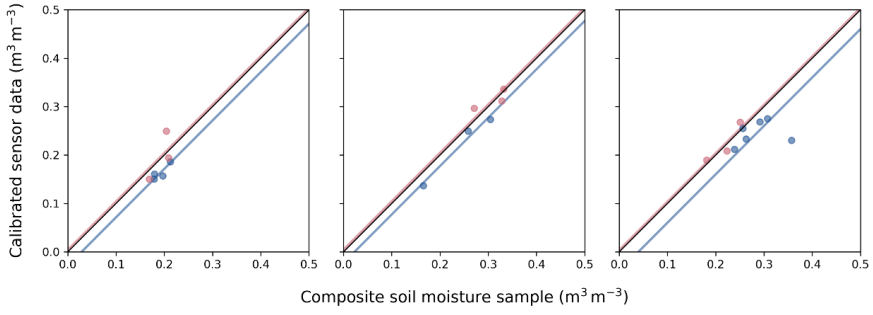

Fig. A2 Examples of double cropping cycles on a certain field within one year that show how the mean bias (intercept) shifts after the sensors are removed and reinstalled (blue: first cropping cycle, pink: second cropping cycle).

665

https://doi.org/10.5194/egusphere-2024-2943
Preprint. Discussion started: 22 October 2024

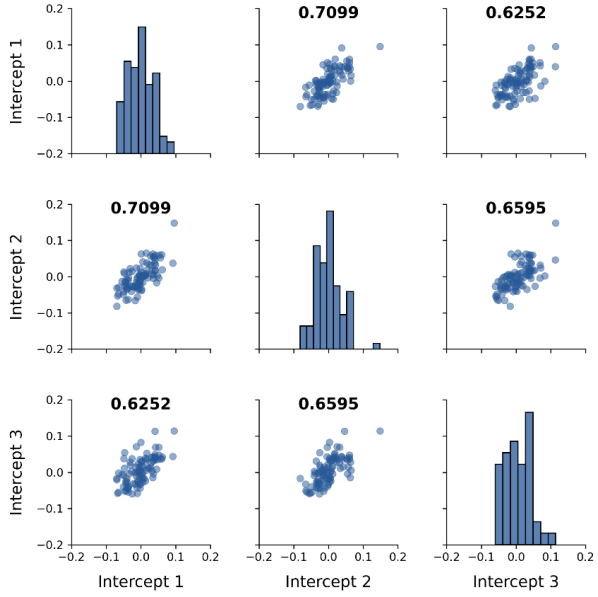

Fig. A3 Pairplot of the three sensor-specific intercepts of each cropping cycle with their Pearson correlations indicated in bold.

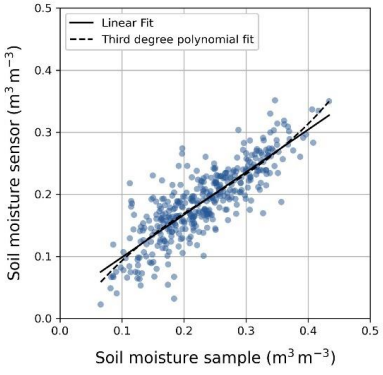

Fig. A4 If we would not opt for an orthogonal Deming regression, but instead fit a model with the soil moisture sensor data being the uncertain dependent variable (*y*) and the soil moisture sample data (ground-truth) being the independent variable (*x*), we can compare different models using the Akaike Information Criterion (AIC). To determine whether a higher-degree polynomial fit would be more appropriate, we tested a second-, third- and fourth-degree polynomial model. The best polynomial model was a third-degree fit with AIC = -1571.6, while the linear model was similar and even slightly better with AIC = -1572.3. The linear regression model and the third-degree polynomial model are plotted.

https://doi.org/10.5194/egusphere-2024-2943
Preprint. Discussion started: 22 October 2024

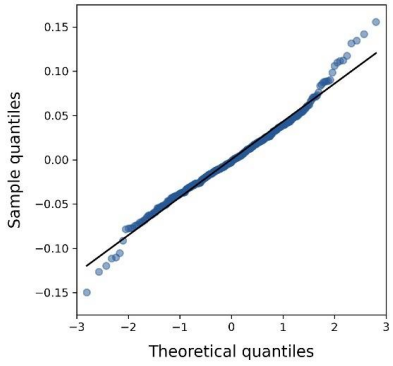

Fig. A5 Normal QQ plot of error residuals

680

https://doi.org/10.5194/egusphere-2024-2943
Preprint. Discussion started: 22 October 2024

Appendix B: Derivation of Eq. (23) and (27)

For n random variables $(X_1, X_2, \dots, X_n)$, the variance of their average is given by Eq. (B1).

$$\mathrm{Var}\left(\frac{X_1+X_2+\cdots+X_n}{n}\right) = \frac{1}{n^2}\mathrm{Var}(X_1 + X_2 + \cdots + X_n)\ . \tag{B1}$$

If the covariances between these variables are equal, i.e., $\mathrm{Cov}_{XX} = \mathrm{Cov}(X_1, X_2) = \cdots = \mathrm{Cov}(X_{n-1}, X_n)$, the variance of the sum of the variables is given by Eq. (B2).

$$\mathrm{Var}(X_1 + X_2 + \cdots + X_n) = \mathrm{Var}(X_1) + \mathrm{Var}(X_2) + \cdots + \mathrm{Var}(X_n) + (n-1)n\mathrm{Cov}_{XX}\ . \tag{B2}$$

If the variances of these variables are also equal, i.e., $\sigma^2 = \mathrm{Var}(X_1) = \mathrm{Var}(X_2) = \cdots = \mathrm{Var}(X_n)$, the variance of the average $(\sigma^2_{\mathrm{mean}})$ can be written as Eq. (B3).

$$\sigma^2_{\mathrm{mean}} = \frac{1}{n^2}[n\sigma^2 + (n-1)n\rho\sigma^2]\ , \tag{B3}$$

where ρ is the correlation, defined as $\frac{\mathrm{Cov}_{XX}}{\sigma^2}$. When both the variance of the n individual variables (σ^2) and the variance of their average $(\sigma^2_{\mathrm{mean}})$ are known, the correlation can be quantified using Eq. (B4).

$$\rho = \frac{n\sigma^2_{\mathrm{mean}} - \sigma^2}{(n-1)\sigma^2}\ . \tag{B4}$$

The correlation between measurements of three sensors $(n = 3)$ can then be quantified using Eq. (B5).

$$\rho = \frac{3\sigma^2_{\mathrm{mean}} - \sigma^2}{2\sigma^2}\ . \tag{B5}$$

https://doi.org/10.5194/egusphere-2024-2943
Preprint. Discussion started: 22 October 2024

Code availability

Python scripts are available upon request.

Data availability

Hendrickx, Marit, 2024, "In situ soil moisture measurement data for sensor calibration and measurement error modeling", https://doi.org/10.48804/M6WKTN, KU Leuven RDR, DRAFT VERSION
(Will be published once the paper gets appointed a DOI)

Author contribution

Competing interests

The authors declare that they have no conflict of interest.
Some authors are members of the editorial board of journal SOIL.

Short summary

We developed a method to estimate errors in soil moisture measurements using limited sensors and infrequent sampling. By analyzing data from 93 cropping cycles in agricultural fields in Belgium, we identified both systematic and random errors for our sensor setup. This approach reduces the need for extensive sensor networks and is applicable to agricultural and environmental monitoring, and ensures more reliable soil moisture data, enhancing water management and improving model predictions.